

01 Jan 1976

Predicting Natural Frequencies Of A Hydrodynamically Lubricated Journal Bearing With Constant Oil Supply Pressure

D. C. Edwards

N. Khorzad

Charles L. Edwards

Missouri University of Science and Technology

Follow this and additional works at: https://scholarsmine.mst.edu/mec_aereng_facwork



Part of the [Aerospace Engineering Commons](#), and the [Mechanical Engineering Commons](#)

Recommended Citation

D. C. Edwards et al., "Predicting Natural Frequencies Of A Hydrodynamically Lubricated Journal Bearing With Constant Oil Supply Pressure," *Journal of Manufacturing Science and Engineering, Transactions of the ASME*, vol. 98, no. 3, pp. 980 - 987, American Society of Mechanical Engineers, Jan 1976.

The definitive version is available at <https://doi.org/10.1115/1.3439061>

This Article - Journal is brought to you for free and open access by Scholars' Mine. It has been accepted for inclusion in Mechanical and Aerospace Engineering Faculty Research & Creative Works by an authorized administrator of Scholars' Mine. This work is protected by U. S. Copyright Law. Unauthorized use including reproduction for redistribution requires the permission of the copyright holder. For more information, please contact scholarsmine@mst.edu.

D. C. Edwards

R. & D. Project Engineer,
Fiber Industries, Inc.,
Charlotte, N. C.

N. Khorzad

Assist. Professor,
Tehran Polytechnic,
and Director of Heavy Industry,
IDRO,
Tehran, Iran

C. L. Edwards

Assoc. Professor,
Mechanical Engineering Department,
University of Missouri-Rolla,
Rolla, Mo.
Mem. ASME

Predicting Natural Frequencies of a Hydrodynamically Lubricated Journal Bearing With Constant Oil Supply Pressure

The analytical and experimental investigations reported here deal with the natural frequencies and system behavior of a full journal bearing subjected to a small sinusoidal load superimposed on a large unidirectional static load. The analysis, verified by experimentation, shows that the bearing can be regarded as two independent second-order systems acting perpendicular to each other. The variable coefficients of the equations of motion cause the bearing to behave as an underdamped system for low values of static eccentricity ratio ϵ_0 , and as an overdamped system for intermediate values of ϵ_0 . The bearing tends to be unstable above a particular ϵ_0 . Further analysis is needed to determine the effects resulting from changing the oil inlet pressure.

Introduction

Most previous work involving the dynamic analysis of journal bearings predicts the motion of the journal center, due to a constant-magnitude rotating-load vector, [1, 2, 3].¹ This loading is applicable to problems such as shaft whirl.

The investigation reported here deals with the first and second natural frequencies of a full journal bearing subjected to a small sinusoidal load superimposed on a large unidirectional static load. Conceding that partial bearings are used, railroad car journals serve as an example, since they may carry a large static load together with a dynamic load due to track joints.

The solution of Reynolds' Hydrodynamic Film Equation as developed by Warner [4] was used to obtain the equations of motion which contain inertial, damping, and elastic characteristics of the lubricant film. Experimental tests, in the form of frequency response, were compared to the analytical solution.

Other aspects of the problem, such as film pressure fluctuation, are to be reported later.

Analytical Development

It can be shown that a general form of Reynolds differential equation for journal bearings is

$$\frac{1}{r^2} \frac{\partial}{\partial \phi} \left[\frac{h^3}{\mu} \frac{\partial P}{\partial \phi} \right] + \frac{\partial}{\partial Z} \left[\frac{h^3}{\mu} \frac{\partial P}{\partial Z} \right] = \frac{6}{r} \frac{\partial}{\partial \phi} (U_1 h) - 12V_1 \quad (1)$$

The right-hand side of equation (1) is a function of ϕ alone, and equation (1) can be written as (see Fig. 1)

$$\frac{1}{r^2} \frac{\partial}{\partial \phi} \left[\frac{h^3}{\mu} \frac{\partial P}{\partial \phi} \right] + \frac{\partial}{\partial Z} \left[\frac{h^3}{\mu} \frac{\partial P}{\partial Z} \right] = 12c \frac{d\epsilon}{dt} \cos \phi - 6(\omega - 2\frac{d\psi}{dt})c\epsilon \sin \phi \quad (2)$$

As can be seen, equation (2) is a nonhomogeneous second order partial differential equation, and the exact solution for it is quite complicated, if not impossible, in explicit form. Warner [4] presented an approximate analytical solution using separation of variables to reduce equation (2) to two ordinary differential equations:

$$\frac{d}{d\phi} \left(\frac{h^3}{\mu} \frac{dF}{d\phi} \right) = r^2 [12c\epsilon \cos \phi - 6(\omega - 2\dot{\psi})c\epsilon \sin \phi] \quad (3)$$

and

$$\frac{\mu}{h^3 r^2} \frac{d}{d\phi} \left(\frac{h^3}{\mu} \frac{dg}{d\phi} \right) + \frac{d^2 g}{dZ^2} = 0 \quad (4)$$

where F and g are functions of ϕ and g is a function of Z only. Equation (4) could be written as

$$\frac{d^2 g}{dZ^2} - \lambda^2 g = 0 \quad (5)$$

and

¹ Numbers in brackets designate References at end of paper.

Contributed by the Design Engineering Division and presented at the Design Engineering Technical Conference, Washington, D. C., September 17-19, 1975, of THE AMERICAN SOCIETY OF MECHANICAL ENGINEERS. Manuscript received at ASME Headquarters, May 27, 1975. Paper No. 75-DET-72.

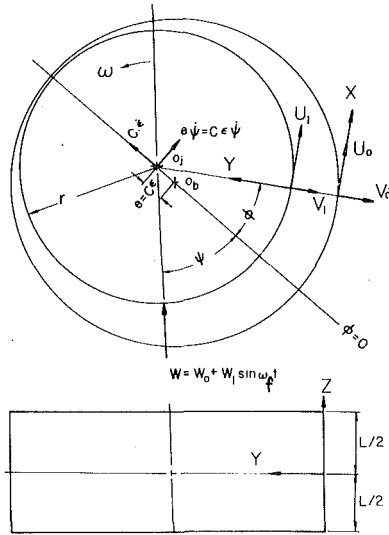


Fig. 1 Full journal bearing coordinate systems

$$\frac{d}{d\phi} \left(\frac{h^3}{\mu} \frac{dg}{d\phi} \right) + (\lambda r)^2 \frac{h^3}{\mu} g = 0 \quad (6)$$

where λ is an eigenvalue, which can be determined from equation (6). Therefore the solution to equation (2) is

$$P(\phi, Z) = \left[1 - \frac{g_1(Z)}{g_1(L/2)} \right] F(\phi) \quad (7)$$

Equation (7) is an approximate solution because the coefficient of $F(\phi)$ is the leading term of an infinite series.

Considering the boundary conditions due to film continuity, i.e., $P(0, Z) = P(2\pi, Z) = 0$, the pressure equation becomes

$$P(\phi, Z) = \left[1 - \frac{\cosh(\lambda Z)}{\cosh(\lambda L/2)} \right] [F_a(\phi) + F_b(\phi)] \quad (8)$$

where

$$F_a(\phi) = 12 \left(\frac{r}{c} \right)^2 \mu \dot{\epsilon} [F_1(\phi) + C_1 F_2(\phi) + C_2] \quad (9)$$

and

$$F_b(\phi) = 6 \mu \left(\frac{r}{c} \right)^2 (\omega - 2\dot{\psi}) [F_3(\phi) + C_3 F_2(\phi) + C_4] \quad (10)$$

Table 1

$A = 1 + \epsilon \cos \phi$	$\gamma = \frac{\epsilon + \cos \phi}{1 + \epsilon \cos \phi}$	$B = 1 - \epsilon^2$
		$\delta = 1$ if $\sin \phi \geq 0$ -1 if $\sin \phi < 0$
$F_1(\phi) = \int \frac{\sin \phi \, d\phi}{A^3} = \frac{1}{2\epsilon A^2}$		
$F_2(\phi) = \int \frac{d\phi}{A^3} = \frac{1}{2B} \left[\frac{-\epsilon \sin \phi}{A^2} - \frac{3\epsilon \sin \phi}{A \cdot B} + \frac{\delta(2 + \epsilon^2)}{B^{3/2}} \cos^{-1} \gamma \right]$		
$F_3(\phi) = \int \frac{d\phi}{A^2} = \frac{1}{B} \left[\frac{-\epsilon \sin \phi}{A^2} + \frac{\delta}{B^{1/2}} \cos^{-1} \gamma \right]$		
$F_4(\phi) = \int F_1 \cos \phi \, d\phi = \frac{1}{2B} \left[\frac{\sin \phi}{\epsilon A} - \frac{\delta}{B^{1/2}} \cos^{-1} \gamma \right]$		
$F_5(\phi) = \int F_2(\phi) \cos \phi \, d\phi = \frac{1}{2B} \left[\frac{B + 3\epsilon A \cos \phi}{\epsilon \cdot A \cdot B} + \frac{(\delta - 1)(2 + \epsilon^2)}{\epsilon B} \right. \\ \left. + \log_e A + \frac{\delta(2 + \epsilon^2)}{B^{3/2}} \cos^{-1} \gamma \right]$		
$F_6(\phi) = \int F_3(\phi) \cos \phi \, d\phi = \frac{1}{B} \left[\cos \phi + \frac{(\delta - 1)}{\epsilon} \log_e A \right. \\ \left. + \frac{\delta \sin \phi}{B^{1/2}} \cos^{-1} \gamma \right]$		
$F_7(\phi) = \int F_1(\phi) \sin \phi \, d\phi = \frac{1}{2\epsilon^2 A}$		
$F_8(\phi) = \int F_2(\phi) \sin \phi \, d\phi = \frac{1}{2B} \left[\frac{(2 + \epsilon^2 + 3\epsilon \cos \phi) \sin \phi}{A \cdot B} \right. \\ \left. + \frac{\delta [2B - A(2 + \epsilon^2)]}{B^{3/2}} \cos^{-1} \gamma \right]$		
$F_9(\phi) = \int F_3(\phi) \sin \phi \, d\phi = \frac{1}{B} \left[\sin \phi + \frac{\delta(B - A)}{\epsilon \cdot B^{1/2}} \cos^{-1} \gamma \right]$		
$F_{10}(\phi) = \int \frac{d\phi}{A} = \frac{\delta}{B^{1/2}} \cos^{-1} \gamma$		
$F_{11}(\phi) = \int \frac{\sin^2 \phi}{A^3} \, d\phi = \frac{1}{\epsilon^2} \left[-BF_2(\phi) + 2F_3(\phi) - F_{10}(\phi) \right]$		
$F_{12}(\phi) = \int \frac{\sin \phi}{A^2} \, d\phi = \frac{1}{\epsilon A}$		

The C 's are integral constants, and F_1, F_2, \dots etc., are given in Table 1.

By evaluating the given functions for a full journal bearing, the pressure equation becomes

Nomenclature

a_c = circumferential acceleration of lubricant in the film
 a_j = radial acceleration of journal center
 a_z = axial acceleration of lubricant in the film
 a_1, a_2 = real parts of complex roots of frequency equation
 B_{xx}, B_{yy} = damping coefficients in x and y direction, respectively
 B_{xy}, B_{yx} = cross damping coefficients
 b_1, b_2 = imaginary parts of complex roots of frequency equation
 c = radial clearance
 D = journal diameter
 e = journal eccentricity (Fig. 1)
 $F(\phi)$ = function of ϕ (Table 1)
 $F'(\phi)$ = function of ϕ (Table 2)
 F_x, F_y = film forces in x and y direction
 g = orthogonal function from equation (7)
 h = film thickness
 K_{xx}, K_{yy} = spring coefficient in x and y direction, respectively

K_{xy}, K_{yx} = cross spring coefficient
 L = bearing length
 M_{xx}, M_{yy} = inertia coefficient in x and y direction, respectively
 M_{xy}, M_{yx} = cross inertia coefficients
 O_b = bearing center
 O_j = journal center
 $P(\phi, z)$ = hydrodynamic film pressure
 $P_a(\phi, z)$ = pressure in the film due to acceleration
 P_0 = film pressure at $\phi = 0$
 P_s = supply pressure
 q = function of z only
 r = journal radius
 r_1, \dots, r_4 = negative real roots of frequency equation
 S = roots of frequency equation
 t = time
 U_1, V_1 = velocities of a point on the journal surface in x and y direction, respectively
 u_j, v_j = coordinate system fixed on bearing

center
 W = bearing load
 W_0 = bearing static load
 W_1 = amplitude of dynamic load
 W_p = force due to film pressure
 x, y, z = coordinate system fixed on center of journal at steady state
 X, Y, Z = coordinate system (see Fig. 1)
 β = bearing arc length
 ϵ = eccentricity ratio = e/c
 ϵ_0 = eccentricity ratio at $t = 0$
 ζ = damping ratio
 η = side leakage factor
 μ = lubricant viscosity, reyns
 ϕ = coordinate measured from line of centers
 ψ = attitude angle, rad (see Fig. 1)
 ψ_0 = attitude angle for static load, W_0
 ω = journal angular velocity
 ω_f = dynamic load frequency
 ω_n = natural frequency

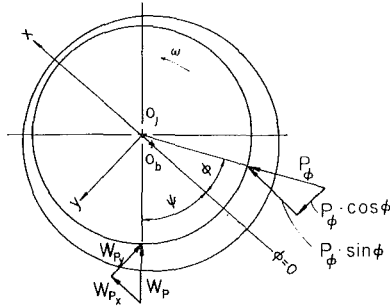


Fig. 2 Pressure force

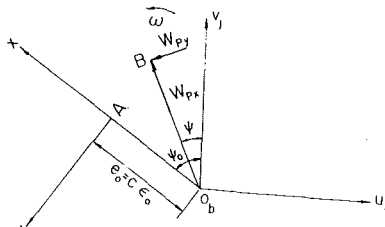


Fig. 3 Displacement due to dynamic forces

$$P(\phi, Z) = \left[1 - \frac{\cosh(\lambda Z)}{\cosh(\lambda L/2)} \right] \left[6 \left(\frac{r}{c} \right)^2 \mu \right] \left\{ \epsilon^2 \left[\frac{1}{\epsilon(1 + \epsilon \cos \phi)^2} - \frac{1}{\epsilon(1 + \epsilon^2)^2} \right] + (\omega - 2\dot{\Psi}) \left[\frac{\epsilon \sin \phi (2 + \epsilon \cos \phi)}{(2 + \epsilon^2)(1 + \epsilon \cos \phi)^2} \right] \right\} + P_0 \quad (11)$$

where, from Fig. (1)

$$h = c(1 + \epsilon \cos \phi) \quad (12)$$

was used to develop equation (11).

Pressure Forces. For now it is assumed that all the load carried by the bearing, identified as W_p , may be determined from the pressure distribution $P(\phi, Z)$. Later other load terms will be added due to dynamic effects.

From Fig. 2:

$$W_{px} = - \int_{-L/2}^{L/2} \int_0^{2\pi} P(\phi, Z) r \cos \phi d\phi dZ \quad (13)$$

$$W_{py} = - \int_{-L/2}^{L/2} \int_0^{2\pi} P(\phi, Z) r \sin \phi d\phi dZ \quad (14)$$

Substituting the value of $P(\phi, Z)$ and integrating

$$W_{px} = -6rL \left(\frac{r}{c} \right)^2 \mu \eta \left\{ 2\epsilon [F_4(\phi) + C_1 F_5(\phi) + C_2 \sin \phi] + (\omega - 2\dot{\Psi}) [F_6(\phi) + C_3 F_5(\phi) + C_4 \sin \phi] \right\} \quad (15)$$

and

$$W_{py} = 6rL \left(\frac{r}{c} \right)^2 \mu \eta \left\{ 2\epsilon [F_7(\phi) + C_1 F_8(\phi) - C_2 \cos \phi] + (\omega - 2\dot{\Psi}) [F_9(\phi) + C_3 F_8(\phi) - C_4 \cos \phi] \right\} \quad (16)$$

where η is an oil side-leakage factor for load:

$$\eta = \left[1 - \frac{\tanh(\frac{\lambda L}{2})}{\lambda L/2} \right] \quad (17)$$

Dynamic Forces.

(i) *Forces Due to Displacement of Journal Center.* In Fig. 3 point A represents the location of the journal center at steady-state with ϵ_0, Ψ_0 as eccentricity ratio and attitude angle, respectively. The coordinate system (x, y) , where the x -axis is along the line

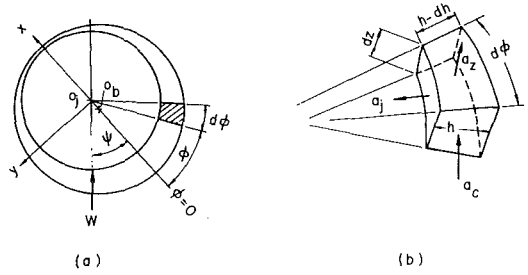


Fig. 4 Film element

of centers, has its origin at point A. Point B is the new position of the journal center slightly displaced from point A. Coordinate system (u_i, v_j) has its origin fixed on the bearing center.

Considering forces due to displacement from equilibrium position A to B with respect to coordinate system (x, y)

$$F_x = W_{px} \cos(\Psi_0 - \Psi) + W_{py} \sin(\Psi_0 - \Psi) \quad (18)$$

$$F_y = W_{px} \sin(\Psi_0 - \Psi) + W_{py} \cos(\Psi_0 - \Psi) \quad (19)$$

Note from Fig. (3) that

$$\Psi = \Psi_0 + \frac{y}{e} \text{ and } \epsilon = \epsilon_0 + \frac{x}{c} \quad (20)$$

Also, assuming a small displacement from point A to B,

$$\sin(\Psi_0 - \Psi) = 0, \cos(\Psi_0 - \Psi) = 1 \quad (21)$$

Expanding equation (18) and equation (19) by Taylor's series about (ϵ_0, Ψ_0)

$$F_x(\epsilon, \Psi) = F_x(\epsilon_0, \Psi_0) + K_{xx}x + K_{xy}y \quad (22)$$

and

$$F_y(\epsilon, \Psi) = F_y(\epsilon_0, \Psi_0) + K_{yx}x - K_{yy}y \quad (23)$$

where

$$K_{xx} = \frac{1}{c} \frac{\partial W_{px}}{\partial \epsilon} - \left[\frac{\partial W_{px}}{\partial \Psi} - W_{py} \right] \frac{y}{e^2} \quad (24)$$

$$K_{xy} = \frac{1}{c\epsilon} \left[\frac{\partial W_{px}}{\partial \Psi} - W_{py} \right] \quad (25)$$

$$K_{yx} = \frac{1}{c} \frac{\partial W_{py}}{\partial \epsilon} - \left[\frac{\partial W_{py}}{\partial \Psi} + W_{px} \right] \frac{y}{e^2} \quad (26)$$

$$K_{yy} = \frac{1}{c\epsilon} \left[W_{px} + \frac{\partial W_{py}}{\partial \Psi} \right] \quad (27)$$

By neglecting higher-order terms, the elastic coefficients will be

$$K_{xx} = -6L\eta\mu \left(\frac{r}{c} \right)^3 \omega \left[\frac{\partial F_6}{\partial \epsilon} + C_3 \frac{\partial F_5}{\partial \epsilon} + F_5 \frac{\partial C_3}{\partial \epsilon} + \frac{\partial C_4}{\partial \epsilon} \sin \phi \right]_0^{2\pi} \quad (28)$$

$$K_{xy} = -6L\eta\mu \left(\frac{r}{c} \right)^3 \frac{\omega}{\epsilon} \left[F_5 \frac{\partial C_3}{\partial \Psi} + \frac{\partial C_4}{\partial \Psi} \sin \phi - F_9 - C_3 F_8 + C_4 \cos \phi \right]_0^{2\pi} \quad (29)$$

$$K_{yx} = 6L\eta\mu \left(\frac{r}{c} \right)^3 \omega \left[\frac{\partial F_3}{\partial \epsilon} + \frac{\partial C_3}{\partial \epsilon} F_8 + C_3 \frac{\partial F_8}{\partial \epsilon} - \frac{\partial C_4}{\partial \epsilon} \cos \phi \right]_0^{2\pi} \quad (30)$$

$$K_{yy} = -6L\eta\mu \left(\frac{r}{c} \right)^3 \frac{\omega}{\epsilon} \left[F_6 + C_3 F_5 + C_4 \sin \phi + \frac{\partial C_3}{\partial \Psi} F_8 - \frac{\partial C_4}{\partial \Psi} \cos \phi \right]_0^{2\pi} \quad (31)$$

(ii) *Forces Due to Velocity of the Journal Center.* By taking the time derivative of equations (20) and assuming small motions

$$\dot{\epsilon} = \frac{\dot{x}}{c}, \quad \dot{\psi} = \frac{\dot{y}}{e} \quad (32)$$

The velocity vector of the journal center, caused by moving the journal center from A to B in Fig. 3, generates forces in the oil film. Equation (32) is substituted into equations (18) and (19) using the approximation of equation (21):

$$F_x = B_{xx}\dot{x} + B_{xy}\dot{y} \quad (33)$$

$$F_y = B_{yx}\dot{x} + B_{yy}\dot{y} \quad (34)$$

where the damping coefficients are

$$B_{xx} = -12L\eta\mu\left(\frac{r}{c}\right)^3 [F_4 + C_1F_5 + C_2 \sin\phi]_0^{2\pi} \quad (35)$$

$$B_{yy} = 12L\eta\mu\left(\frac{r}{c}\right)^3 \frac{1}{\epsilon} [F_6 + C_3F_5 + C_4 \sin\phi]_0^{2\pi} \quad (36)$$

$$B_{yx} = -12L\eta\mu\left(\frac{r}{c}\right)^3 [F_7 + C_1F_8 - C_2 \cos\phi]_0^{2\pi} \quad (37)$$

$$B_{yy} = 12L\eta\mu\left(\frac{r}{c}\right)^3 [F_9 + C_3F_8 - C_4 \cos\phi]_0^{2\pi} \quad (38)$$

(iii) *Forces Due to Acceleration of Journal Center.* Evaluation of the acceleration terms will necessitate taking the inertia of the lubricant into account. The inertia of the journal was considered and found to be small relative to the effect of the lubricant inertia.

Acceleration applied on the running journal will produce a sudden change in the pressure of the film. The lubricant in the film is accelerated circumferentially and axially in making way for the journal. There is also radial acceleration of the film, but since it is of smaller order compared to the axial and circumferential components, it is neglected.

In Fig. 4(b), a_j is the radial acceleration of the journal, a_c the circumferential acceleration, and a_z the axial acceleration of lubricant at angle ϕ . From the continuity equation

$$a_j = \frac{1}{r} \frac{\partial}{\partial \phi} (\dot{a}_c h) + h \frac{\partial a_z}{\partial z} \quad (39)$$

The general form of Navier-Stokes equation [5] consists of an inertia term, pressure gradient terms, and shear terms. In the derivation of Reynolds' equation inertia is neglected. Therefore, neglecting the shear term and considering the inertia terms, the Navier-Stokes equations reduce to

$$\rho a_c = -\frac{1}{r} \frac{\partial P_a}{\partial \phi} \quad (40)$$

$$\rho a_z = -\frac{\partial P_a}{\partial z} \quad (41)$$

Substituting equations (40), (41), and (12) into equation (39), and writing a_j in terms of its components of the x, y coordinate system

$$\frac{1}{r} \frac{\partial}{\partial \phi} [1 + \epsilon \cos\phi] \frac{\partial P_a}{\partial \phi} + (1 + \cos\phi) \frac{\partial^2 P_a}{\partial z^2} = \frac{\rho}{c} [a_x \cos\phi + a_y \sin\phi] \quad (42)$$

where a_x and a_y are components of a_j in the x - and y -directions, respectively.

Due to the similarity of form between equation (42) and equation (2), the pressure distribution due to acceleration will be

$$P_a(\phi, z) = \frac{\cosh(\lambda_a z)}{\cosh(\lambda_a L/2)} \frac{\rho r^2}{c \epsilon} \left\{ a_x \log_e \left(\frac{1 + \epsilon}{1 + \epsilon \cos\phi} \right) + a_y [(2\pi - \phi) + \cos^{-1} \left(\frac{\epsilon + \cos\phi}{1 + \epsilon \cos\phi} \right)] \right\} \quad (43)$$

where λ_a is the eigenvalue calculated from the solution of equation (42). Forces due to $P_a(\phi, z)$ can be given as

Table 2

$A = 1 + \epsilon \cos \phi$	$\gamma = \frac{\epsilon + \cos \phi}{1 + \epsilon \cos \phi}$	$B = 1 - \epsilon^2$
		$\delta = 1$ if $\sin \phi \geq 0$ -1 if $\sin \phi \leq 0$
$F_1'(\phi) = \int \frac{d\phi}{\lambda} = \frac{\delta}{B^{1/2}} \cos^{-1} \gamma$		
$F_2'(\phi) = \int \frac{\sin \phi d\phi}{\lambda} = -\frac{1}{\epsilon} \log_e \lambda$		
$F_3'(\phi) = \int \frac{\cos \phi d\phi}{\lambda} = \frac{1}{\epsilon} [-F_1'(\phi) + \phi]$		
$F_4'(\phi) = \int F_1'(\phi) \sin \phi d\phi = \frac{\delta}{B^{1/2}} \left[\cos \phi \cos^{-1} \gamma - \frac{\delta}{\epsilon} \cos^{-1} \gamma + \frac{\phi}{\epsilon B^{1/2}} \right]$		
$F_5'(\phi) = \int F_1'(\phi) \cos \phi d\phi = \frac{\delta}{B^{1/2}} \left[\sin \phi \cos^{-1} \gamma + \frac{B^{1/2}}{\epsilon} \log_e \lambda \right]$		
$F_6'(\phi) = \int F_2'(\phi) \sin \phi d\phi = \frac{1}{\epsilon} \left[(\cos \phi + \frac{1}{\epsilon}) \log_e \lambda - \cos \phi \right]$		
$F_7'(\phi) = \int F_2'(\phi) \cos \phi d\phi = -\frac{\sin \phi}{\epsilon} \log_e \lambda + \frac{\delta B^{1/2}}{\epsilon^2} \cos^{-1} \gamma$		
$F_8'(\phi) = \int F_3'(\phi) \sin \phi d\phi = \frac{1}{\epsilon} [-F_4'(\phi) + \sin \phi - \phi \cos \phi]$		
$F_9'(\phi) = \int F_3'(\phi) \cos \phi d\phi = \frac{1}{\epsilon} [-F_5'(\phi) + \phi \sin \phi + \cos \phi]$		

$$W_{ax} = M_{xx}\ddot{x} + M_{xy}\ddot{y} \quad (44)$$

$$W_{ay} = M_{yx}\ddot{x} + M_{yy}\ddot{y} \quad (45)$$

where in general form

$$M_{xx} = \frac{r^3 L \rho \eta a}{C} \left\{ [F_1'(\phi)]_{\phi_1}^{\phi_1+\beta} - \frac{[F_2'(\phi)]_{\phi_1}^{\phi_1+\beta}}{[F_1'(\phi)]_{\phi_1}^{\phi_1+\beta}} [F_5'(\phi)]_{\phi_1}^{\phi_1+\beta} + [-F_2'(\phi_1 + \beta) + \frac{[F_2'(\phi)]_{\phi_1}^{\phi_1+\beta}}{[F_2'(\phi)]_{\phi_1}^{\phi_1+\beta}}] \times F_1'(\phi_1 + \beta) [\sin\phi]_{\phi_1}^{\phi_1+\beta} \right\} \quad (46)$$

$$M_{xy} = -\frac{r^3 L \rho \eta a}{C} \left\{ [F_9'(\phi)]_{\phi_1}^{\phi_1+\beta} + \frac{[F_3'(\phi)]_{\phi_1}^{\phi_1+\beta}}{[F_1'(\phi)]_{\phi_1}^{\phi_1+\beta}} \times [F_5'(\phi)]_{\phi_1}^{\phi_1+\beta} + [F_3'(\phi_1 + \beta) - \frac{[F_3'(\phi)]_{\phi_1}^{\phi_1+\beta}}{[F_1'(\phi)]_{\phi_1}^{\phi_1+\beta}}] \times F_1'(\phi_1 + \beta) [\sin\phi]_{\phi_1}^{\phi_1+\beta} \right\} \quad (47)$$

$$M_{yx} = \frac{r^3 L \rho \eta a}{C} \left\{ [F_6'(\phi)]_{\phi_1}^{\phi_1+\beta} - \frac{[F_2'(\phi)]_{\phi_1}^{\phi_1+\beta}}{[F_1'(\phi)]_{\phi_1}^{\phi_1+\beta}} \times [F_4'(\phi)]_{\phi_1}^{\phi_1+\beta} + [F_2'(\phi_1 + \beta) - \frac{[F_2'(\phi)]_{\phi_1}^{\phi_1+\beta}}{[F_1'(\phi)]_{\phi_1}^{\phi_1+\beta}}] \times F_1'(\phi_1 + \beta) [\cos\phi]_{\phi_1}^{\phi_1+\beta} \right\} \quad (48)$$

$$M_{yy} = \frac{r^3 L \rho \eta a}{C} \left\{ -[F_8'(\phi)]_{\phi_1}^{\phi_1+\beta} + \frac{[F_3'(\phi)]_{\phi_1}^{\phi_1+\beta}}{[F_1'(\phi)]_{\phi_1}^{\phi_1+\beta}} \times [F_4'(\phi)]_{\phi_1}^{\phi_1+\beta} - [F_3'(\phi_1 + \beta) - \frac{[F_3'(\phi)]_{\phi_1}^{\phi_1+\beta}}{[F_1'(\phi)]_{\phi_1}^{\phi_1+\beta}}] [F_1'(\phi_1 + \beta) + \beta] [\cos\phi]_{\phi_1}^{\phi_1+\beta} \right\} \quad (49)$$

For a full journal bearing, $\phi_1 = 0, \beta = 2\pi$ and

$$\eta_a = \left[1 - \frac{\tanh\left(\frac{\lambda_a L}{2}\right)}{\lambda_a L/2} \right] \quad (50)$$

F_s are given in Table 2.

General Equation. Assuming that the principle of superposition applies, the equation of motion can be written by adding equations (22), (23), (33), (34), (44), and (45):

External load Steady-state
load force

$$\begin{aligned} \begin{Bmatrix} W_x \\ W_y \end{Bmatrix} &= \begin{Bmatrix} F_x(\epsilon_0, \Psi_0) \\ F_y(\epsilon_0, \Psi_0) \end{Bmatrix} + \\ &\underbrace{\text{Dynamic forces}} \\ &+ \begin{bmatrix} K_{xx} & K_{xy} \\ K_{yx} & -K_{yy} \end{bmatrix} \begin{Bmatrix} x \\ y \end{Bmatrix} + \begin{bmatrix} B_{xx} & B_{xy} \\ -B_{yx} & -B_{yy} \end{bmatrix} \begin{Bmatrix} \dot{x} \\ \dot{y} \end{Bmatrix} \\ &+ \begin{bmatrix} M_{xx} & M_{xy} \\ -M_{yx} & -M_{yy} \end{bmatrix} \begin{Bmatrix} \ddot{x} \\ \ddot{y} \end{Bmatrix} \quad (51) \end{aligned}$$

For an external load shown in Fig. 1

$$W = W_0 + W_1 \sin \omega_f t$$

$$W_x = W \cos \Psi_0 \quad W_y = W \sin \Psi_0$$

Also

$$F_x(\epsilon_0, \Psi_0) = W_0 \cos \Psi_0, \quad F_y(\epsilon_0, \Psi_0) = W_0 \sin \Psi_0$$

Frequency Equation

General Case. Equation (51) may be written in the form

$$\begin{Bmatrix} \ddot{x} \\ \ddot{y} \end{Bmatrix} + \begin{bmatrix} B_1 & B_3 \\ A_3 & A_1 \end{bmatrix} \begin{Bmatrix} \dot{x} \\ \dot{y} \end{Bmatrix} + \begin{bmatrix} B_2 & B_4 \\ A_4 & A_2 \end{bmatrix} \begin{Bmatrix} x \\ y \end{Bmatrix} = \begin{Bmatrix} B_5 \\ A_5 \end{Bmatrix} \quad (52)$$

where x is the horizontal displacement and y is the vertical displacement of the journal center with respect to the bearing center.

Desiring only the characteristic or frequency equation for the bearing, load terms B_5 and A_5 are ignored. Equation (52) in operator form yields

$$(D^2 + B_1 D + B_2)x + (B_3 D + B_4)y = 0 \quad (53)$$

$$(A_3 D + A_4)x + (D^2 + A_1 D + A_2)y = 0 \quad (54)$$

The frequency equation becomes

$$\begin{aligned} S^4 + (A_1 + B_1)S^3 + (A_2 + B^2 + A_1 B_1 - A_3 B_3)S^2 \\ + (A_1 B_2 + A_2 B_1 - A_3 B_4 - A_4 B_3)S + (A_2 B_2 - A_4 B_4) = 0 \quad (55) \end{aligned}$$

The form of the roots of equation (55) depends on static eccentricity ratio ϵ_0 as follows:

1 Two conjugate pairs for small ϵ_0

$$S_{1,2} = (-\zeta_1 \pm i\sqrt{1 - \zeta_1^2})\omega_{n1} \quad (56)$$

$$S_{3,4} = (-\zeta_2 \pm i\sqrt{1 - \zeta_2^2})\omega_{n2} \quad (57)$$

2 Two real roots and one conjugate pair for intermediate ϵ_0

$$r_{1,2} = (-\zeta_1 \pm \sqrt{\zeta_1^2 - 1})\omega_{n1} \quad (58)$$

$$S_{3,4} = (-\zeta_2 \pm i\sqrt{1 - \zeta_2^2})\omega_{n2} \quad (59)$$

3 Four real roots for large ϵ_0

$$r_{1,2} = (-\zeta_1 \pm \sqrt{\zeta_1^2 - 1})\omega_{n1} \quad (60)$$

$$r_{3,4} = (-\zeta_2 \pm \sqrt{\zeta_2^2 - 1})\omega_{n2} \quad (61)$$

Specific Case. Equation (55) was solved using a journal bearing with the following parameters:

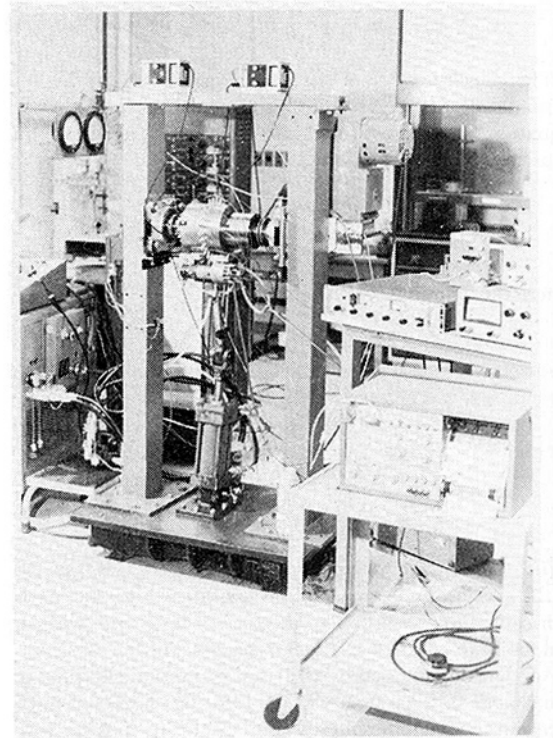


Fig. 5 General view of apparatus

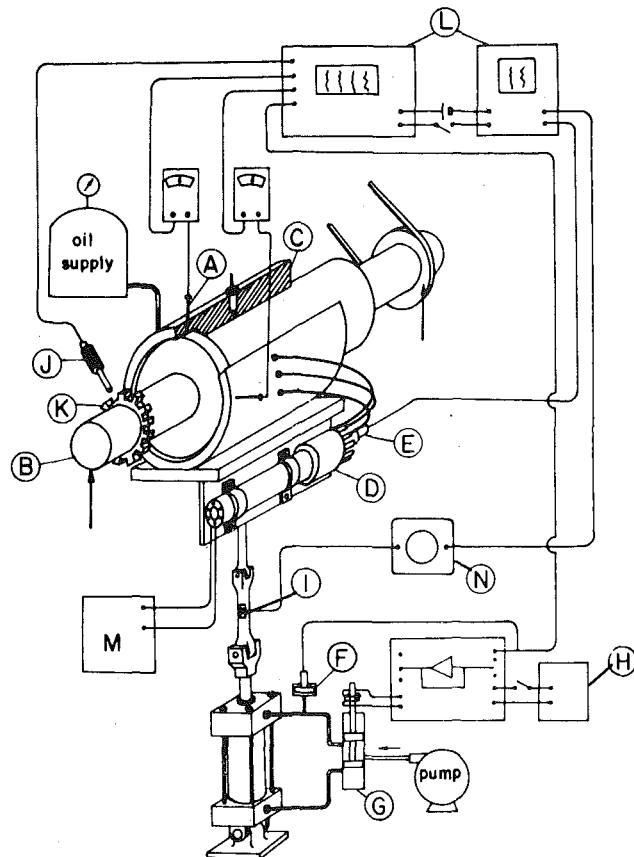


Fig. 6 Schematic of apparatus: A—proximity sensors, B—journal, C—bearing, D—scanning valve, E—pressure transducer, F—feed-back pressure transducer, G—servo-valve, H—oscillator, I—strain gage, J—magnetic sensor, K—timing gear, L—recorders, M—scanning valve control panel, N—amplifier

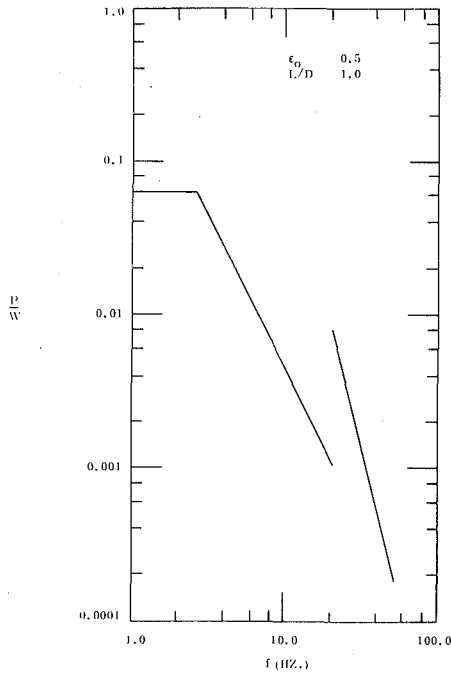


Fig. 7 Frequency response of bearing

$$\begin{aligned}
 L &= D = 127.0 \text{ mm (5.0 in.)} \\
 C &= 0.065 \text{ mm (0.00255 in.)} \\
 \mu &= 0.0168 \text{ Pa}\cdot\text{s (2.44} \times 10^{-6} \text{ reyns)} \\
 P_s &= 138 \text{ kPa (20 psig)}
 \end{aligned}$$

For small values of ϵ_0 the bearing behaved as an underdamped system with roots as in equations (56) and (57). At $\epsilon_0 = 0.575$ the roots took the form of equations (58) and (59). When $\epsilon_0 = 0.655$ was reached the roots were those of equations (60) and (61). Higher values of ϵ_0 yielded positive real roots from equation (55). Since this implies that the system is unstable [6], the analysis was terminated.

Experimental Work

The parameters of the journal bearing are the same as those given in the previous section. The complete test apparatus is shown in Fig. 5 and a corresponding schematic is shown in Fig. 6. The method of load application and measuring bearing displacement and pressure in the oil film are also shown in Fig. 6.

Twenty-three equally spaced 1-mm dia holes drilled radially through the bearing were used to measure pressure in the oil film. Oil was supplied to the bearing through one of the holes, which was enlarged, and connected to an oil reservoir pressurized to 138 kPa (20 psig) and held constant. The load was applied to the loading block beneath the journal bearing through a hydraulic cylinder and tie rod.

With the journal rotating at the desired speed, the static load W_0 was applied and the system allowed to stabilize at ϵ_0 . The dynamic load, $W_1 \sin \omega t$, was applied, with the magnitude W_1 as close to 10 percent of W_0 as possible.

Two types of frequency response were found. The first was the ratio of maximum film pressure P to total load W , and the second, the ratio of displacement to W . For both types of response, the load W_0 was adjusted so that the eccentricity ratio ϵ_0 was constant over the range of forcing frequencies.

Proximity devices, Fig. 6, were used to measure the relative displacement of bearing and journal. Through a transformation [7], displacements could be found in the x - and y -directions, Fig. 2. These transducers could also be used to verify the eccentricity ratio ϵ_0 .

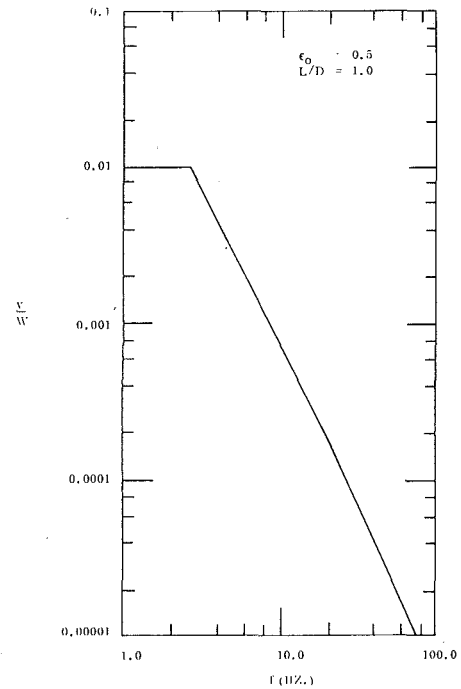


Fig. 8 Frequency response in y -direction

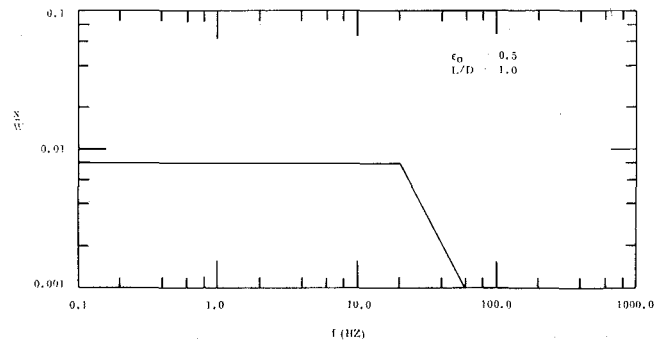


Fig. 9 Frequency response in x -direction

Discussion

Fig. 7 shows a typical response curve of the bearing in terms of maximum film pressure P and total load W . This loading was chosen ($\epsilon_0 = 0.5$) because both break-points could be reached experimentally. The break-points occur at 2.6 Hz (16.3 rad/s) and 21 Hz (132 rad/s) which are quite close to the values of ω_{n1} and ω_{n2} at $\epsilon_0 = 0.5$ from Figs. 10 and 11, respectively. The slope of Fig. 7 beyond ω_{n1} is approximately two log units per decade while the slope after ω_{n2} is about 3.6 log units per decade. This indicates that the bearing behaved similar to two second-order systems superimposed on each other.

Frequency response in terms of displacement is shown in Figs. 8 and 9. Fig. 8 shows a break-point occurring in the y -direction at 2.6 Hz, and Fig. 9 a break-point in the x -direction at 21 Hz. Since the loading is the same ($\epsilon_0 = 0.5$) they may be compared to Fig. 7, which has the same break-points.

Experimental and analytical values for ω_{n1} and ω_{n2} are shown in Figs. 10 and 11. Fig. 11 shows only analytical values for ω_{n2} , although ω_{n2} was found experimentally for $\epsilon_0 = 0.5$, as previously discussed. However, other values of ω_{n2} were not found due to the difficulty and even impossibility of the system to operate at such high frequencies. The system was limited by the frequency response to the hydraulic cylinder.

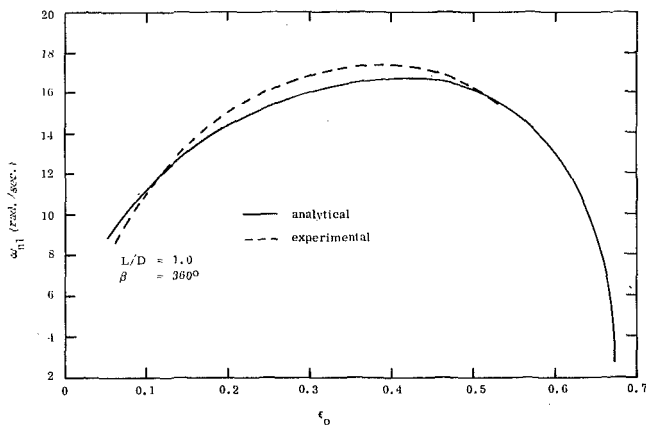


Fig. 10 ω_{n1} versus ϵ_0

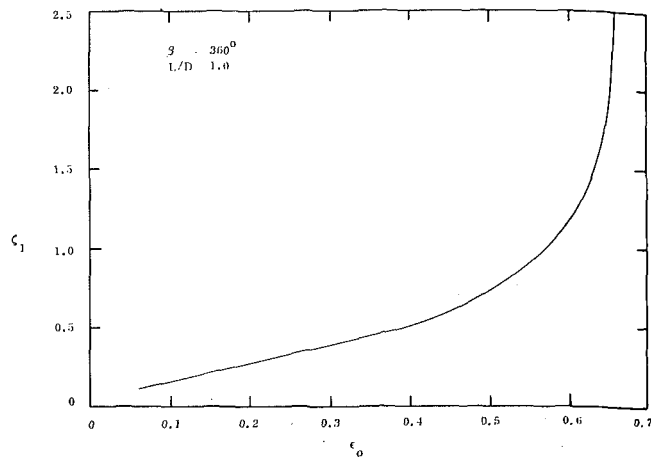


Fig. 12 Damping ratio corresponding to ω_{n1}

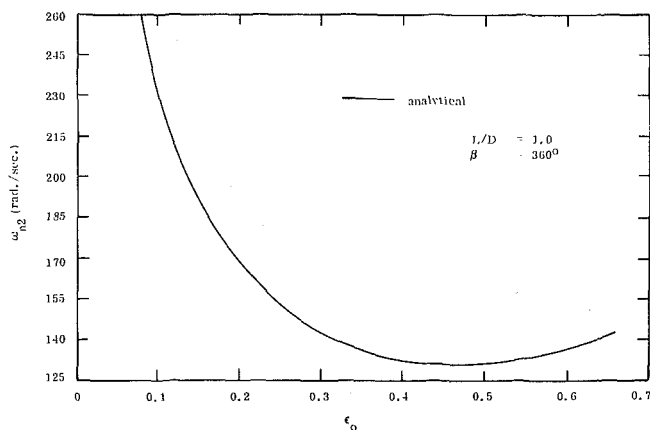


Fig. 11 ω_{n2} versus ϵ_0

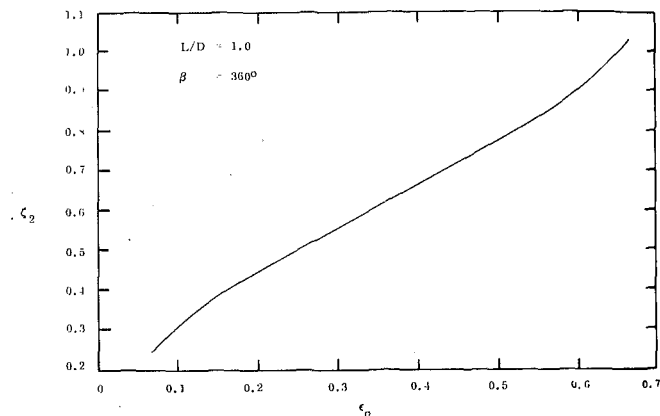


Fig. 13 Damping ratio corresponding to ω_{n2}

Figs. 10 and 11 show that natural frequency can be found in terms of ϵ_0 . It is important to recall that ϵ_0 depends on the Sommerfeld number which, in part, depends on journal load and angular velocity. A given bearing has a predictable relation between eccentricity ratio and Sommerfeld number. But the same Sommerfeld number and thus the same eccentricity ratio is realized as long as the ratio of journal angular velocity to journal load is constant. This is limited by the ability of the system to conform to its mathematical model. When other phenomena such as excessive shaft deflection, foaming, or cavitation are predominant, the model fails.

Figs. 12 and 13 show the corresponding damping ratios, ζ_1 and ζ_2 , for Figs. 10 and 11, respectively. Fig. 12 shows a tremendous increase in ζ_1 beyond $\epsilon_0 = 0.6$ for this particular bearing. When this region is compared to Fig. 10 it is evident that ω_{n1} is approaching zero. A natural frequency equal to zero yields a "rigid-body" mode. This means metal-to-metal contact between journal and bearing due to a breakdown in the hydrodynamic oil film. Therefore, once a certain ϵ_0 is reached (0.675 in this case), the bearing starts to make contact with the journal and gradually begins to wear. Increased loading just speeds up the wearing process.

Figs. 12 and 13 also indicate the transition of the bearing from an underdamped ($\zeta < 1.0$) to an overdamped ($\zeta > 1.0$) system. From Fig. 12 critical damping, in the first mode of vibration, occurs at $\epsilon_0 = 0.575$, and from Fig. 13 the second mode is critically damped at $\epsilon_0 = 0.655$ for this particular bearing.

Fig. 14 shows how ϵ and ψ vary with respect to time when the bearing is operating at ω_{n1} . The bearing eccentricity ratio increased while ψ , the attitude angle, decreased. Fig. 2 shows that if ψ decreased to zero then the line of centers would be vertical. Therefore Fig. 14 shows that most of the vibration occurs in the y , i.e., vertical direction. If the bearing were operated at ω_{n2} , it is as-

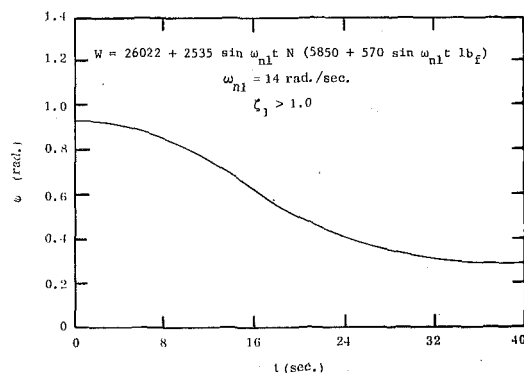
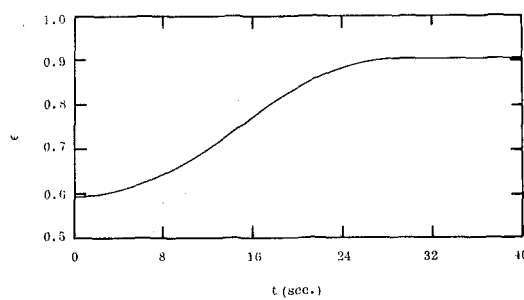


Fig. 14 Transient response of bearing at ω_{n1}

sumed that ψ would approach 90 deg and most of the vibration would be in the horizontal (x) direction.

The fact that ω_{n1} and ω_{n2} are widely separated (Figs. 10 and 11) tempts us to regard the bearing as two separate systems, one for the x -direction and another for the y -direction. Therefore uncoupling equation (52) yields

$$\ddot{y} + A_1 \dot{y} + A_2 y = 0 \quad (62)$$

$$\ddot{x} + B_1 \dot{x} + B_2 x = 0 \quad (63)$$

where

$$A_1 = 2\zeta_1 \omega_{n1}, \quad A_2 = \omega_{n1}^2 \quad (64)$$

$$B_1 = 2\zeta_2 \omega_{n2}, \quad B_2 = \omega_{n2}^2 \quad (65)$$

Equations (62)-(65) can then be used to yield first and second modes of the bearing with reasonable accuracy.

References

- 1 Harrison, W. J., "The Hydrodynamical Theory of the Lubrication of a Cylindrical Bearing Under Variable Load, and of a Pivot Bearing," *Cambridge Philosophical Society*, Vol. 22, 1920, pp. 373.
- 2 Swift, H. W., "Fluctuating Loads in Sleeve Bearings," *Journal of the Institution of Civil Engineers* (London), Vol. 5, 1937, pp. 161-195.
- 3 Dick, J., "Alternating Loads on Sleeve Bearings," *Philosophical Magazine* (London), Vol. 35, 1944, pp. 841-850.
- 4 Warner, P. C., "Static and Dynamic Properties of Partial Journal Bearings," *Journal of Basic Engineering*, TRANS. ASME, Vol. 85, June 1963, pp. 274-275.
- 5 Tuan, S. W., *Foundation of Fluid Mechanics*, Prentice-Hall, Englewood Cliffs, N. J., 1967.
- 6 Vierck, R. K., "Two-Degree-of-Freedom Systems," *Vibration Analysis*, International, Scranton, 1967, pp. 206-209.
- 7 Khorzad, N., "A Study of the Dynamic Loading of Hydrodynamically Lubricated Journal Bearings," Doctor of Philosophy thesis, University of Missouri-Rolla, Appendix I, 1973, pp. 84-87.